



Wear properties of CrC–37WC–18M coatings deposited by HVOF and HVAF spraying processes

I. Hulka^a, V.A. Şerban^a, I. Secoşan^a, P. Vuoristo^{b,*}, K. Niemi^b

^a Department of Materials and Welding Science "Politehnica" University of Timișoara, Blv. Mihai Viteazu, No 1, RO-300222, Romania

^b Department of Materials Science, Tampere University of Technology, Korkeakoulunkatu 6, FI-33101 Finland

ARTICLE INFO

Article history:

Received 30 March 2012

Accepted in revised form 29 July 2012

Available online 4 August 2012

Keywords:

CrC–37WC–18M

HVOF

HVAF

Wear

ABSTRACT

CrC–37WC–18M cermet coatings were deposited using new feedstock powders which seem to combine the properties of WC–CoCr and CrC–NiCr coatings. A conventional particle size CrC–37WC–18M powder was used as feedstock for the HVOF (high velocity oxygen fuel) thermal spraying process and a fine particle distribution was used as feedstock for the HVAF (high velocity air fuel) thermal spraying process. In order to characterize the morphology of the feedstock powders and deposited coatings SEM and X-ray diffraction were used. The microhardness of the coatings was also studied. The wear behavior of the coatings was evaluated by pin-on-disk and rubber wheel abrasion tests. The HVAF coating showed equal or even better wear resistance as compared to corresponding HVOF coatings.

© 2012 Elsevier B.V. All rights reserved.

1. Introduction

Thermal sprayed WC cermet coatings have been used to resist wear environments at ambient and elevated temperatures for a number of years due to their properties such as high abrasion, sliding and erosion resistance, advantages offered by dense coatings [1,2]. High velocity oxygen fuel (HVOF) thermal spraying is suitable in obtaining dense cermet coatings with low oxidation due to its unique advantage of heating the feedstock to near or above its melting point, preferably between the solidus and liquidus temperatures, at a relatively low process temperature by a supersonic combustion gas stream [3–5]. Due to high velocity, the time of interaction between the powder and the flame shortens and in conjunction with the process temperature limited thermal alteration occurs ensuring good cohesion and morphology with reduced porosity and low decarburization [6,7]. An alternative to the HVOF process, for manufacturing cermet hard coatings, is the high velocity air fuel (HVAF) process which utilizes compressed air, instead of oxygen, for combustion and operates at lower temperatures than the HVOF process [8]. The HVAF process reduces the manufacturing cost of coatings, replacing pure oxygen by compressed air having as consequence coatings which do not show any of the oxidation or decarburization effects after spraying [9]. WC and Cr_xC_y based thermally sprayed coatings are extensively used to decrease the friction coefficient between various sliding components and to improve corrosion resistance in many industries [10,11]. Due to the Cr content the coatings are suitable for

high-temperature applications [12]. The CrC–37WC–18M is quite a new powder developed to combine the properties of WC–CoCr and CrC–NiCr cermet powders. It is composed of two carbide phases WC and Cr₃C₂ embedded into an alloy composed of Ni, Co and a small amount of Fe. There are no studies in the literature focused on the properties of CrC–37WC–18M deposited via HVOF and HVAF processes. The aim of the study was to characterize the phase and microstructure of the CrC–37WC–18M coatings deposited by HVAF and HVOF thermal spraying as well as to study the composition, abrasive and sliding wear behaviors of the coatings.

2. Experimental

Two types of CrC–37WC–18M powders were used for this study: a WOKA 7502 powder with a nominal size distribution of $-45 + 15 \mu\text{m}$ and a fine WOKA 7504 powder with a nominal size distribution of $-30 + 10 \mu\text{m}$. Both powders are manufactured by Sulzer Metco, Germany, by agglomeration and sintering. A Sympatec Helos laser diffractometer was used to determine the particle size distribution of the powders. Philips XL-30 scanning electron microscope equipped with an EDAX analyzer was used to investigate the morphology of the powders and coatings in this study. WOKA 7504 powder was deposited by the HVAF process using a M2 thermal spray gun with 0.52 [MPa] propane, respectively and [0.59] MPa air as process gases. The standoff distance was 150 mm. WOKA 7502 powder was deposited by the HVOF process using a Diamond Jet Hybrid 2700 gun at TUT with 68 l/min propane, 236 l/min oxygen and 368 l/min air as process gases. The standoff distance was 230 mm, traverse speed of the gun 11 mm/s and powder feed rate 60 g/min. This gun provides particle velocities up to 650 m/s. In both processes nitrogen was used as a carrier gas for the feedstock

* Corresponding author. Tel.: +358 40 849 0044; fax: +358 3 3115 2330.

E-mail addresses: hulka_iosif@yahoo.com (I. Hulka), viorel.serban@rectorat.upt.ro (V.A. Şerban), ionut_secosan@yahoo.com (I. Secoşan), petri.vuoristo@tut.fi (P. Vuoristo), kari.niemi@tut.fi (K. Niemi).

Table 1

Particle size distribution and chemical composition in weight [%] [Sulzer Metco, Germany].

Trade name	d ₁₀ [μm]	d ₅₀ [μm]	d ₉₀ [μm]	C %	Ni %	Co %	Fe %	Cr %	WC %
WOKA 7502	22.17	37.39	50.09	8.11	11.63	3.63	0.23	40.74	Balance
WOKA 7504	15.77	25.22	34.77	8.16	11.27	3.64	0.22	40.22	Balance

powder, with a 13 l/min flow for the HVOF process. The coatings were deposited on 50×20×4 mm low carbon steel plates and steel disks with a diameter of 65 mm for pin-on-disk tests. To increase the roughness of the substrates, alumina grit was used as an abrasive media in order to increase the bonding strength between the coating and the substrate. The phase composition of powders and coatings was investigated by X-ray diffraction analysis with Cu K α radiation (1.5406 Å) using a 0.02° step size and 0.2 s step time. X-ray diffraction was performed at a tube voltage of 40 kV and a tube current of 30 mA. The X-ray intensity was measured over a 2 θ diffraction angle from 10° to 100°. The porosity was quantified in each coating by image analysis

technique using the Image Tool 3.00 software onto 7 BSE–SEM micrographs at 1000× magnification. A Matsuzava MMT X7 Vickers tester was used to measure the microhardness on the cross-section of the coatings using a load of 300 g and, performing 10 indentations per sample. Abrasion wear resistance of the coatings was evaluated by using the rubber wheel abrasion wear tester using dry quartz sand as an abrasive, with a grain size in the range of 0.1–0.6 mm, on ground samples. The diameter of the rubber wheel was 660 mm, the test load was 22 N and wear losses were measured after every 12 min. Duration of the test was 1 h which equals to the total wear length of 5904 m. Before measurements the samples were blasted with compressed air to remove sand particles left on the samples. After abrasion tests the topography of the coatings was studied using a Veeco Wyko NT1100 optical profiler which provided three-dimensional surface images and more precise roughness measurements. Also SEM was used to observe the worn surfaces and carbide pullouts.

The sliding wear tests were performed using a CETR UMT tribometer on a polished surface with a 0.03 μm Ra final value. Three tests were carried out on each coating. A WC–Co ball with a diameter of 6.3 mm was used as a counter body. The applied normal force was 10 N and the

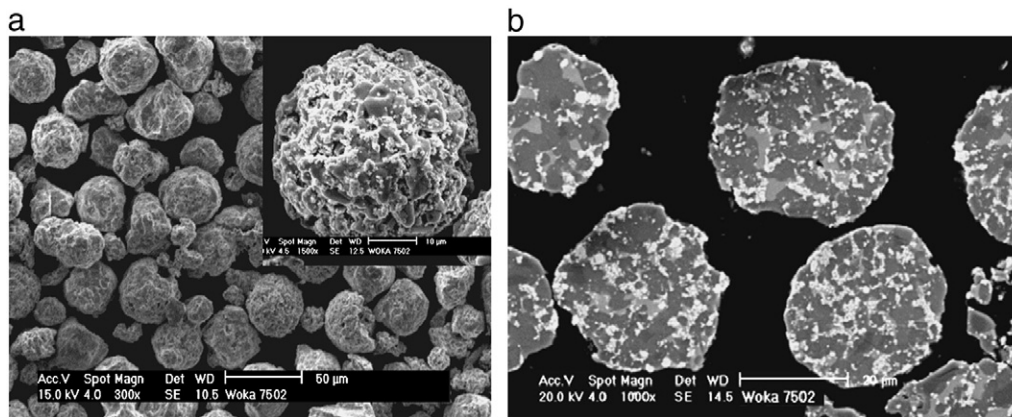


Fig. 1. Morphology of WOKA 7502 powder: a) at 300× (single powder particle at 1500×), b) cross section.

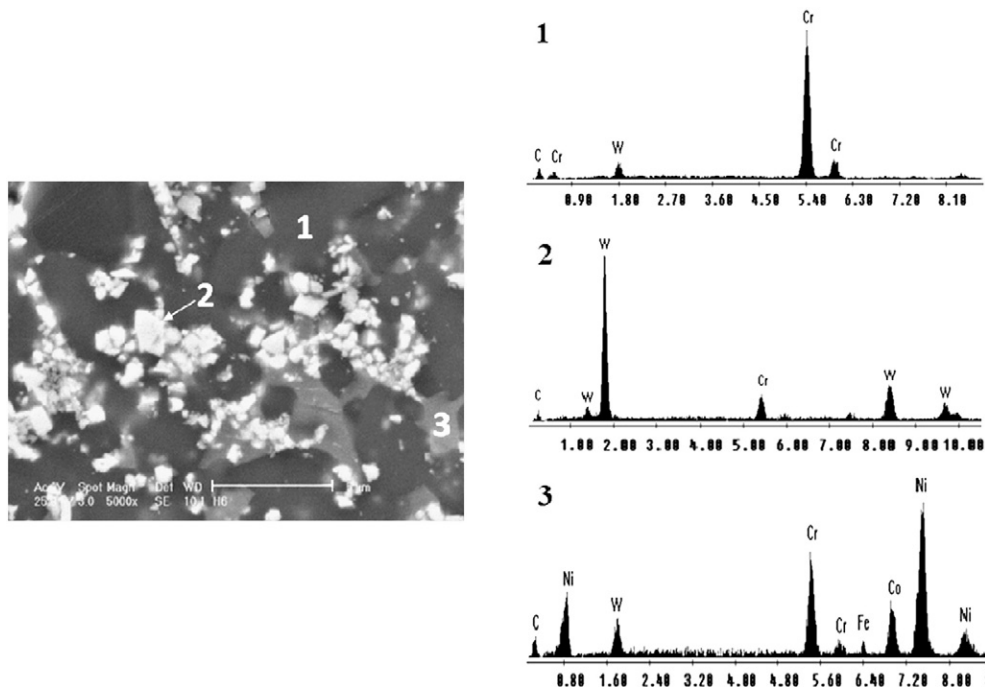


Fig. 2. SEM micrograph at a high magnification and EDX spectra of individual spray particles.

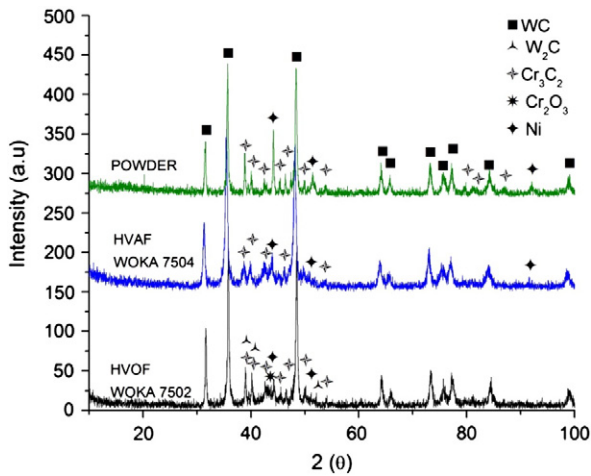


Fig. 3. XRD spectra of feedstock powder, and HVOF and HVOF coatings.

diameter of the wear track was 22 mm. The test speed was 120 rev/min and it was performed on a 3000 m distance at room temperature.

3. Results and discussion

3.1. Powder characterization

The powders obtained by agglomeration and sintering have an improved flow ability due to round shaped powder particles with homogeneous microstructure and prevalent equilibrium phases [13]. In this study the investigated powders have two stable carbide phases WC and Cr_2C_3 which are embedded into a Ni–Co–Fe metallic matrix

which bind together the carbide phases. Table 1 presents the size distribution measurements and the chemical composition of the feedstock powders according to the manufacturer. The large amount of powder particles with sizes above the nominal particle size of both powders might be influenced by the different equipment used by the quality-control measurements of the suppliers. The powders can be treated as identical from the point of view of chemical composition. The powder particles show typical agglomerated and sintered rounded shapes (Fig. 1). In some powder particles, pore entrances and reduced porosity can be observed which is probably due to the manufacturing process, as it can be noticed in the cross section of the powder particle (Fig. 1b). According to EDX analysis (Fig. 2) the dark gray areas (1) represent the Cr_3C_2 carbide phase while the bright areas (2) are rich in W representing the WC phase. The bright gray areas (3) represent the metallic phase which contains all the elements presented in the chemical composition, but the presence of Ni can be noticed. The WC particles were measured by SEM and the grains for the feedstock powders were in the range of 0.25–1.7 μm .

The XRD pattern of the feedstock powder (Fig. 3) indicated the presence of WC phases (JCPDS card 25-1047) and Cr_3C_2 (JCPDS card 35-0804) as main phases in conjunction with amounts of Ni (JCPDS card 01-1258). Due to the fact that the powders are identical with regard to the phase composition only one XRD pattern for the powder WOKA 7502 was presented.

3.2. Coating characterization

SEM micrographs indicated that both coatings have good adherence to the substrate with low amounts of impurities and pores (Fig. 4). The HVOF deposited coating has a thickness of about 270 μm and the HVOF deposited coating 160 μm . The HVOF coating presents a lower degree of porosity due to lower process temperature and high particle velocities.

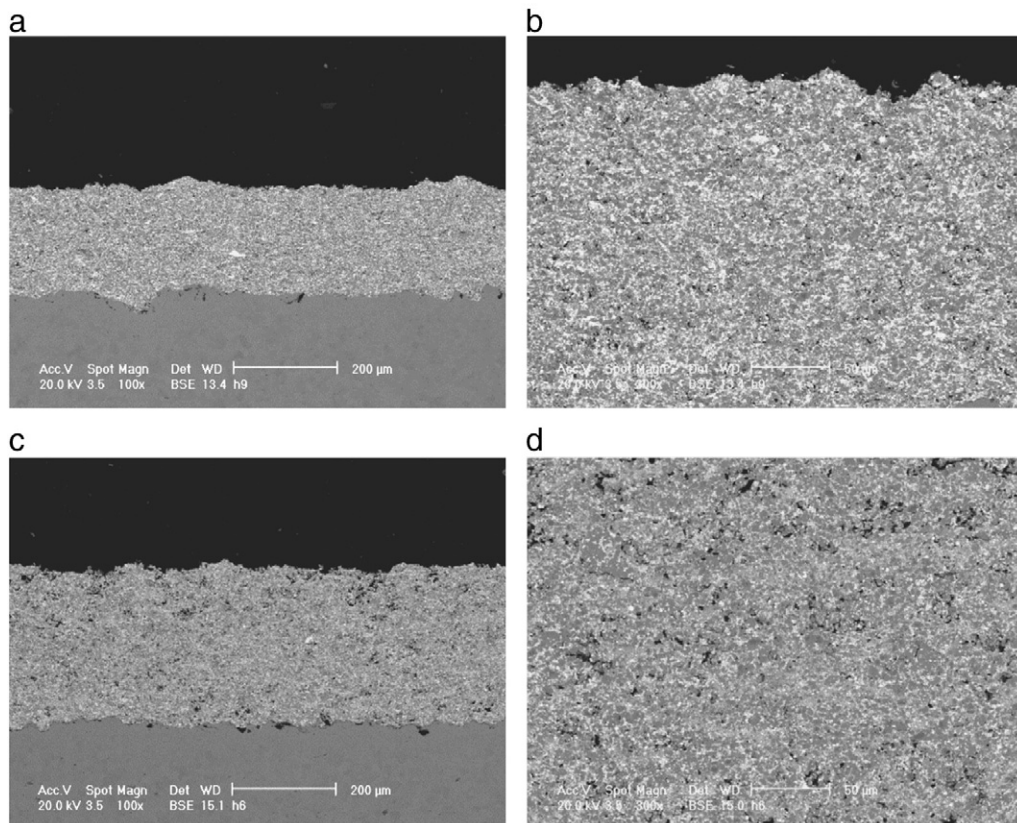


Fig. 4. SEM micrographs at 4000 \times and EDX spectra of the metallic matrix: a) HVOF coating and b) HVOF coating.

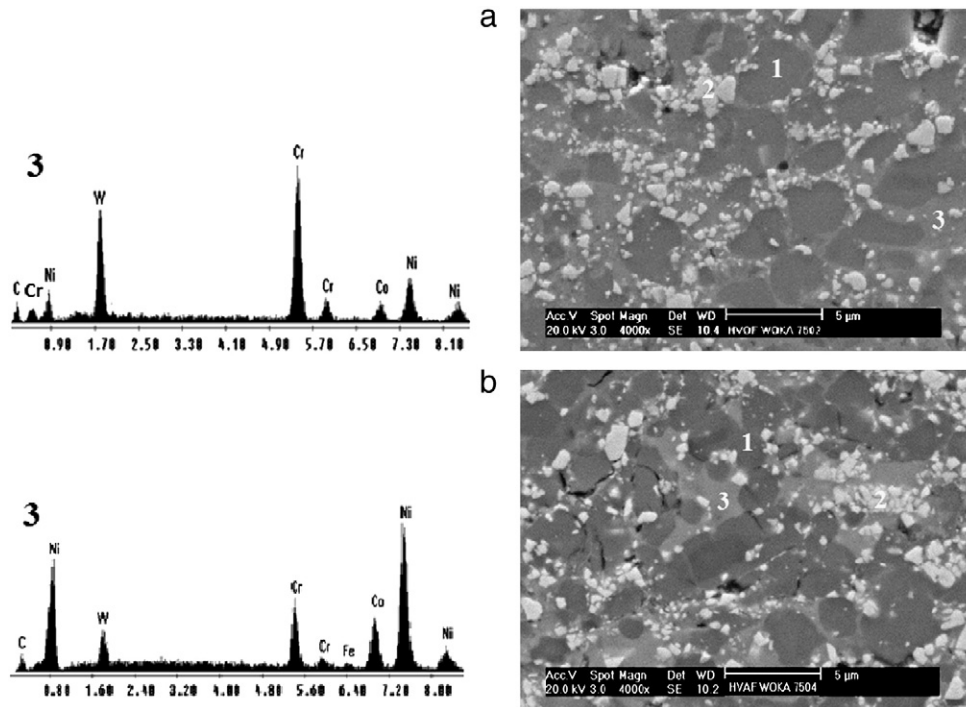


Fig. 5. Cross sectional SEM micrographs of: a) HVOF coating at 100 \times , b) HVOF coating at 300 \times , c) HVAF coating at 100 \times and d) HVAF coating at 300 \times .

According to the porosity quantification the HVOF coating has presented somewhat a higher degree of porosity with 1.63% in comparison with the HVAF coating with 0.92% porosity. This might be caused by the different particle size distributions of the powder and different spraying processes. The roughness values of the as deposited coatings were measured (8 measurements have been performed per coating) using a SJ-301 Mitutoyo tester and the mean results were almost identical, Ra-5.18 μm for the HVAF coating and Ra-5.25 μm for the HVOF coating. The EDX spectra and high magnification SEM micrographs (Fig. 5) proved that the HVAF process did not affect the phase compositions found in the feedstock powder. The presence of WC phases and Cr_2C_3 phases can be noticed in both coatings. The EDX spectrum of the matrix region in the HVOF deposited coating indicates the presence of a much larger amount of Cr which is caused by some interdiffusion between the metallic matrix and the carbide phase (Fig. 5). The XRD pattern (Fig. 3) indicated that the HVAF coating has an identical peak position with the feedstock powder, but the diffraction peaks are

somewhat broader. This might be due to a lower interdiffusion process, in comparison with HVOF sprayed coating, between the chromium carbide phase and metallic matrix, which means that no significant transformation took place during thermal spraying due to the lower spraying temperature. The presence of WC, Cr_3C_2 and Ni phases can be noticed also in the HVOF coating. According to the JCPDS standard the W_2C and Cr_2O_3 phases were also identified. Some other small peaks in the XRD pattern might correspond to Cr_7C_3 or other phases which were hard to identify. The micro-hardness values of the HVAF coating was $932 \pm 47 \text{ HV}_{0.3}$ and the HVOF coating showed somewhat higher hardness values, respectively $1045 \pm 65 \text{ HV}_{0.3}$. The reason for increased hardness in the case of the HVOF coating is the presence of hard but brittle phases which formed during spraying due to the decarburization process. The influence of abrasive media on the grinded coatings (Fig. 6) proved that both coatings have good wear resistance with similar results, but the HVAF coating showed somewhat lower wear loss. The topography of the worn samples (Fig. 7) indicated that the Cr_3C_2

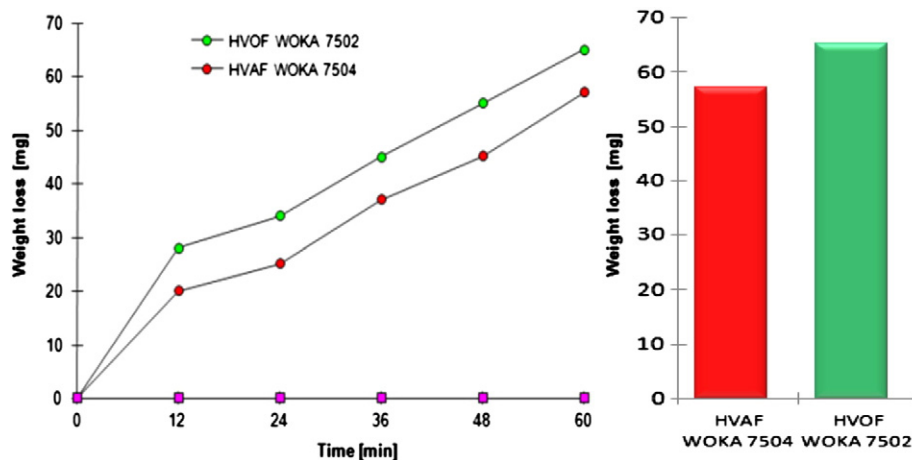


Fig. 6. Abrasion wear results for the sprayed coating.

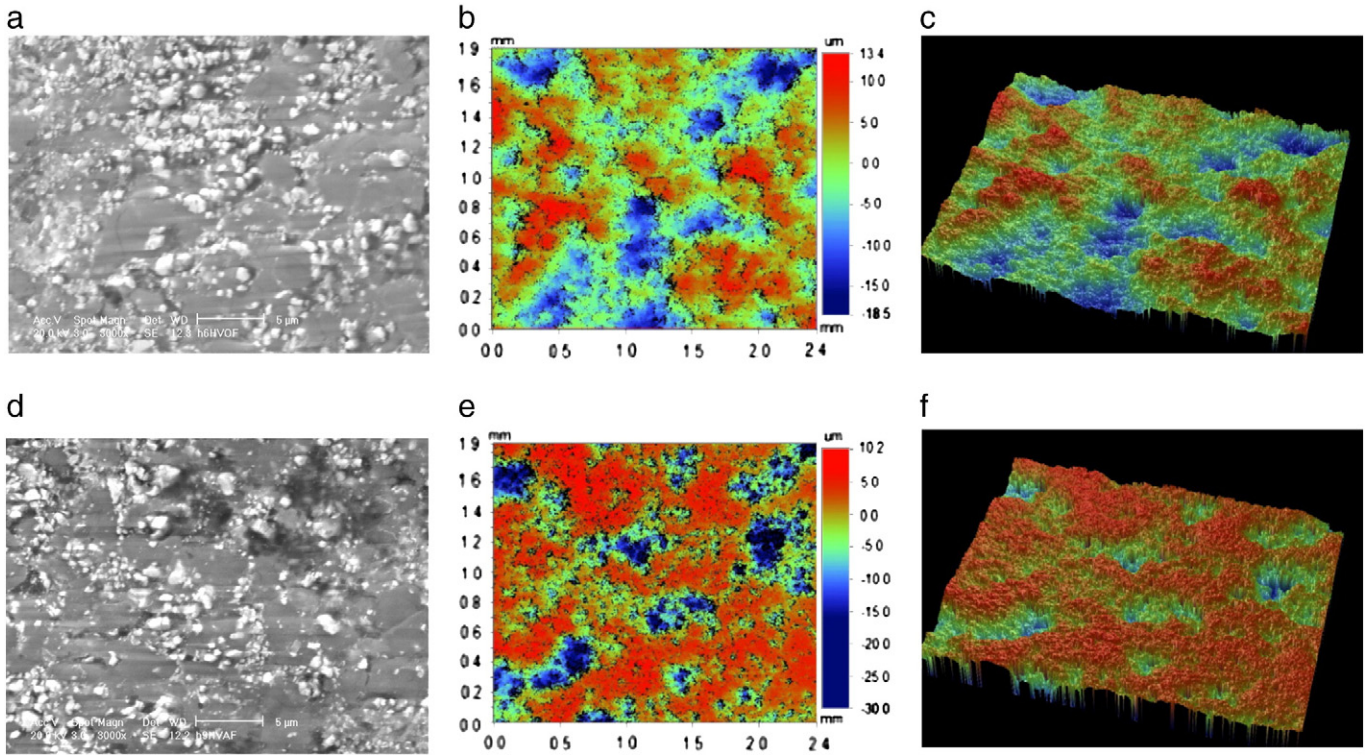


Fig. 7. Topography of HVOF/HVAF coatings after abrasion test: a) HVOF SEM at 4000 \times , b) HVOF 2D image of scanned area, c) HVOF 3D profile of the scanned area, d) HVAF SEM at 4000 \times , e) HVAF 2D image of scanned area and f) HVAF 3D profile of the scanned area.

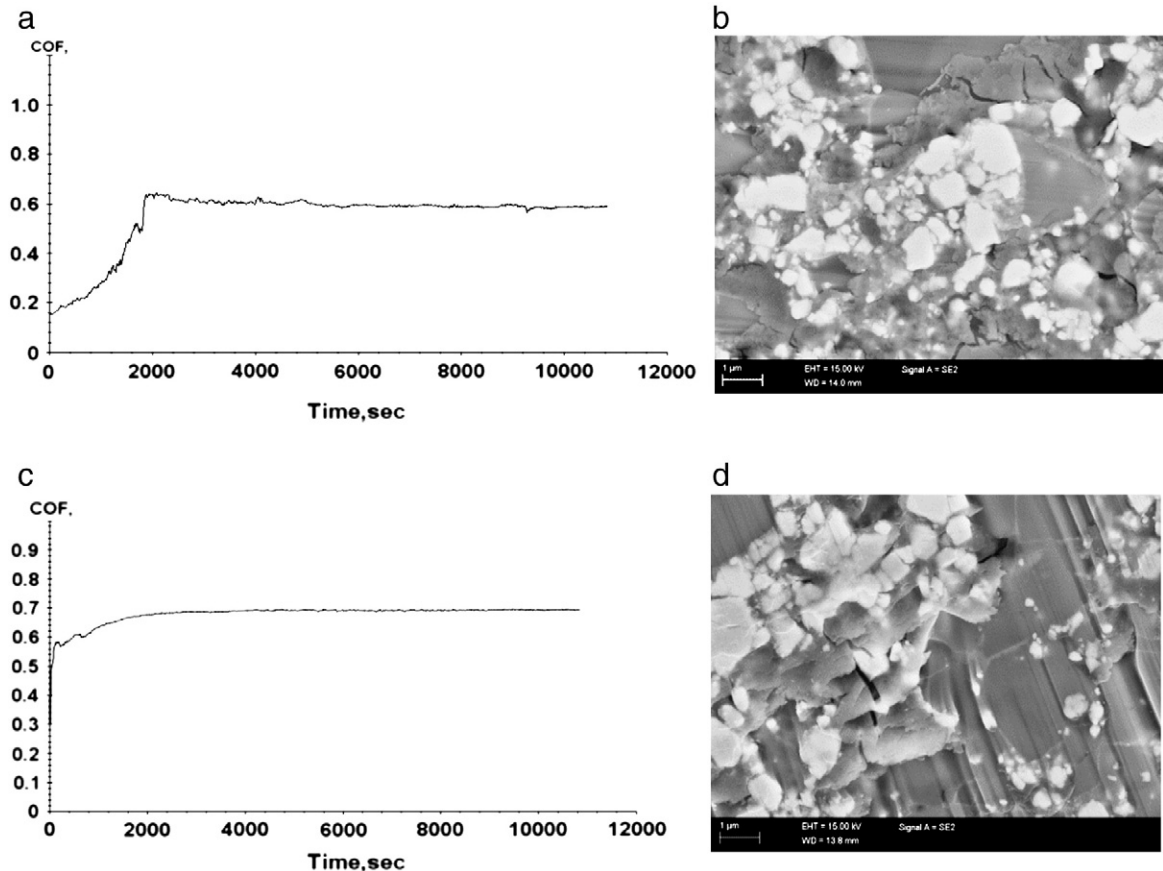


Fig. 8. CoF as a function of sliding time and worn track morphology: a) CoF of HVAF coating, b) worn track morphology of HVAF coating, c) CoF of HVOF coating and d) worn track morphology of HVOF coating.

Table 2
Results of pin-on-disk wear test.

Measurements/coating	HVAF	HVOF
Ball worn cap diameter [μm]	384.2	760.16
Sample wear rate [$\text{mm}^3/\text{N}/\text{m}$]	$2.26 \cdot 10^{-5}$	$2.62 \cdot 10^{-5}$
Ball wear rate [$\text{mm}^3/\text{N}/\text{m}$]	$1.13 \cdot 10^{-8}$	$1.74 \cdot 10^{-7}$

phase and metallic matrix suffered scratches and in time material removal while the WC particles suffered pullouts. Comparing the 2D and 3D images it can be observed that the HVAF coating suffered less material loss during the abrasion test. The measured roughness values, after the abrasion test, have been somewhat lower R_a -3.56 μm for the HVAF coating and somewhat higher, R_a -4.21 μm for the HVOF coating. The sliding test results (Fig. 8) indicate that sliding wear resistance of HVAF sprayed coating was enhanced and the coating exhibited the best wear performance in comparison with HVOF sprayed coating. Due to the high rotation speed and the applied load without lubrication the sliding wear is considered to be mainly adhesive wear. Material removal and formation and propagation of cracks and deeper grooves in the chromium carbide matrix and metallic matrix can be noticed in the HVOF coating while in the HVAF coating the grooves are less deep and WC carbide pull outs can be noticed (Fig. 8b). Detachments of the coating were also formed on both coating worn tracks. The grooves are caused by the detachments of coating, debris particles, which act as an abrasive third body between the coating and counter body. Due to higher oxidation and decarburization formation and propagation of cracks are noticed on the HVOF coating surface. Even the HVAF coating has a lower microhardness, and the non-oxidized coating can effectively retain mechanical strength having a lower wear rate (Table 2).

4. Conclusions

The following conclusions can be drawn from this study:

1. The microstructure of HVAF sprayed CrC–37WC–18M coating is dense and possesses lower porosity in comparison with HVOF coating.

2. Decarburization and oxidation are reduced in the HVAF coating due to lower process temperatures which is confirmed by the XRD pattern confirming the presence of WC, Cr_3C_2 and Ni phases in both coatings, but W_2C and Cr_2O_3 have been identified in the HVOF. There is almost no difference between the HVAF sprayed coating and the feedstock powder which means that no significant transformation took place during the spraying process.
3. During the wear tests, the HVAF coating presented similar or somehow better results than the HVOF coating due to denser coating build up at a lower temperature.

Acknowledgment

This work was partially supported by the strategic grant POSDRU 2009 project ID 50783 of the Ministry of Labor, Family and Social Protection, Romania, co-financed by the European Social Fund-Investing in People. The authors would like to acknowledge FincoatOy, Finland for the HVAF depositions.

References

- [1] B.S. Mann, V. Arya, P. Joshi, J. Mater. Eng. Perform. 14 (4) (2005) 487.
- [2] W. Zórawski, N. Radek, in: B.R. Marple, M.M. Hyland, Y.C. Lau, C.J. Li, R.S. Lima, G. Montavon (Eds.), ITSC 2009, Las Vegas, USA, 2009, p. 1052.
- [3] N. Zeoli, S. Gu, S. Kamnis, Comput. Chem. Eng. 32 (2008) 1661.
- [4] S.H. Zhang, T.Y. Cho, J.H. Yoon, M.X. Li, P.W. Shum, S.C. Kwon, Mater. Sci. Eng., B 162 (2009) 127.
- [5] T.C. Hanson, G.S. Settles, J. Therm. Spray Technol. 12 (3) (2003) 403.
- [6] J.A. Picas, A. Forn, A. Igartua, G. Mendoza, Surf. Coat. Technol. (2003) 1095.
- [7] M. Li, D. Shi, P.D. Christofides, Powder Technol. 165 (2–3) (2005) 177.
- [8] I.A. Grolach, R D J. 25 (2009) 40.
- [9] L. Jacobs, M. Hyland, M. De Bonte, in: Christian Coddet (Ed.), Thermal Spray-Meeting the Challenge of the 21st Century, Vol. 1, Nice, 1998, p. 169.
- [10] M. Prudenziati, G.C. Gazzadi, M. Medici, G. Dalbagni, M. Caliari, Therm. Spray Technol. 19 (2010) 541.
- [11] W. Tillmann, E. Vogli, I. Baumann, G. Kopp, C. Weihs, Therm. Spray Technol. 19 (2010) 392.
- [12] Committee on CoatingsNational Materials Advisory Board, in: National Academy of Science, Washington D.C., 1970, p. 71.
- [13] M. Oechsle, in: Christian Penszior, Peter Heinrich (Eds.), Hochgeschwindigkeits-Flammspritzen/HVOF Spraying, Vol. 8, Erding, 2009, p. 71.